Ann Based Controller for Grid Integration of Hybrid Converterless Microgrid

Sampathirao Nagaraju¹, Dr. Kottala Padma²

¹Department Of Electrical Engineering Andhra University College of Engineering (A) Andhra University Visakhapatnam 2023-2025

²Associate Professor, Department of Electrical Engineering Andhra University College of Engineering
(A) Andhra University Visakhapatnam 2023-2025

Abstract—The increasing demand for clean and sustainable energy has led to the development of advanced hybrid renewable energy systems. This study focuses on the modelling, control, and energy management of a hybrid grid-connected power system that integrates wind energy, photovoltaic (PV) systems, a battery energy storage system (BESS), fuel cells (FC), and an electrolyser. The proposed system configuration eliminates the need for a separate PV converter by combining wind and PV as primary energy sources, BESS as a secondary source, and the combination of FC and electrolyser as tertiary sources. This design not only simplifies the system architecture but also enhances cost-effectiveness and overall reliability.

To achieve optimal performance, a Hybrid Artificial Neural Network (ANN) controller is implemented, which provides adaptive, intelligent, and non-linear control for maintaining system stability and efficient energy flow under variable wind and solar conditions. The system stability is further improved using a lead compensator with an integrator, which minimizes steady-state errors and ensures an appropriate phase margin. The Rotor Side Controller (RSC) and Grid Side Controller (GSC) operate cooperatively to maintain grid synchronization, provide frequency support, and ensure efficient power distribution from renewable sources.

The ANN-based controller effectively compensates for the intermittency and power fluctuations inherent in renewable energy sources by dynamically adjusting power flow between the BESS, FC, and electrolyser. The electrolyser stores excess energy by producing hydrogen during high-generation periods, which is later utilized by the fuel cell during low-generation conditions, thus ensuring continuous power supply. The advanced energy management system also prevents BESS overcharging, minimizes power oscillations, and guarantees a stable power output to the grid.

The proposed ANN-based control technique effectively minimizes oscillations in the DC-link voltage, improves transient response, and enhances the overall system stability when compared to conventional control methods. The simulation results, obtained using MATLAB/Simulink, clearly validate that the ANNbased hybrid system ensures steady power flow, efficient energy management, reduced converter count, and higher overall efficiency under various environmental and operational conditions. In the previously used control method, the system's power output settled between 8.5 to 12 seconds. However, with the implementation of the ANN controller, the power settles at its final steady-state positive value much faster, reaching stability at around 0.35 seconds. This demonstrates a significant improvement in the dynamic performance and response speed of the system.

I. INTRODUCTION

1.1 Overview

The advancement and expansion of electrical power systems face numerous challenges that extend beyond technological limitations include environmental, social, economic, and financial considerations. In the 21st century, climate change and sustainable development have emerged as critical issues affecting energy and environmental security. Conventional energy sources such as coal, oil, and natural gas not only increase the cost of electricity generation but also have detrimental environmental impacts, contributing to pollution and greenhouse gas emissions. The rapid growth in energy demand exacerbates these effects, leading to long-term consequences for the environment. These challenges can be mitigated by adopting renewable energy sources such as wind power, solar photovoltaics

(PV), and tidal energy, which offer sustainable alternatives with minimal environmental impact.

However, renewable sources are inherently intermittent due to climatic variations such as solar irradiance, temperature, and wind speed, which can limit consistent power generation. To address this issue, Hybrid Energy Systems (HES) have been developed, allowing for efficient, reliable, and economical utilization of renewable resources. This approach combines multiple energy sources, along with energy storage and control systems, to ensure a continuous power supply. The project focuses on designing power management and control strategies, as well as testing and validating associated algorithms within a simulated environment. Mathematical modeling plays a crucial role in simulating energy conversion systems, including solar PV and windbased units.

Modern power grids are increasingly incorporating advanced technologies to enhance efficiency, reliability, and flexibility. In this context, microgrids are poised to be a key driver of transformation in electrical infrastructure, supported by technical, economic, and social factors. The declining costs of PV panels and inverters, along with the relatively low cost of natural gas and diesel in certain regions, have made distributed generation comparable to traditional grid power, further motivating the integration of renewable energy sources as a long-term solution.

Globally, there is growing recognition that independent hybrid solar-wind power systems provide a superior alternative for supplying electricity to remote areas where grid connection is not feasible. For example, according to the 2006 Statistics Canada Census, 194,281 people lived in 292 remote settlements that were not connected to the main power grid. These regions possess significant wind energy potential, yet rely primarily on diesel generators, consuming approximately 1,477,415 MWh annually. To reduce both the high operational costs and environmental impact of diesel-based generation, innovative strategies aimed at minimizing diesel usage are essential. Between 2008 and 2011, solar PV generation in Canada grew at an annual rate of 147.3%, while wind energy utilization also increased, with projections indicating it could account for 12% of global electricity generation by 2020.

As a result, the concept of hybrid operation has attracted increasing attention in the power sector. The Techno Centre Éolien (TCÉ) has implemented a hybrid renewable energy system in Gaspé, Quebec, combining a wind power plant, compressed air storage, motor-generator electric drive (MGSet), battery storage, heat exchanger, resistive loads, secondary loads, and remote monitoring systems. The primary objective of such research is to assess the functionality, reliability, and autonomous operation of hybrid energy systems, providing a sustainable solution for power generation in both remote and grid-connected areas.

The proposed ANN-based control technique effectively minimizes oscillations in the DC-link voltage, improves transient response, and enhances the overall system stability when compared to conventional control methods. The simulation results, obtained using MATLAB/Simulink, clearly validate that the ANN-based hybrid system ensures steady power flow, efficient energy management, reduced converter count, and higher overall efficiency under various environmental and operational conditions. In the previously used control method, the system's power output settled between 8.5 to 12 seconds. However, with the implementation of the ANN controller, the power settles at its final steady-state positive value much faster, reaching stability at around 0.35 seconds. This demonstrates a significant improvement in the dynamic performance and response speed of the system.

1.2 Literature Review

The integration of renewable energy sources into electrical grids has become a significant research focus due to the increasing demand for sustainable and environmentally friendly power generation. Conventional energy sources such as coal, oil, and natural gas have detrimental effects on the environment, leading to global efforts to adopt renewable energy technologies, including wind, solar, and hybrid systems. However, renewable energy sources are inherently intermittent and variable, making it challenging to maintain grid stability, voltage regulation, and reliable power supply. To address these challenges, Hybrid Energy Systems (HES) combining multiple renewable sources with energy storage and intelligent control mechanisms have been widely studied.

Wind-Diesel Hybrid Systems have been one of the earliest hybrid configurations explored. Pena-Alzola [1] demonstrated that independent wind-diesel systems can significantly reduce fuel consumption when operated in Wind Only mode, minimizing diesel generator usage. Achieving this mode requires advanced control strategies and energy storage mechanisms, particularly batteries, which reduce the start-stop cycles of diesel generators. Batteries are preferred for short-term storage due to their high efficiency and fast response compared to other storage options. These systems typically use three-phase bridges to interface the battery with the isolated grid, ensuring compliance with power standards.

Hirose and Matsuo [2] proposed a freestanding hybrid system combining wind, solar, battery storage, and diesel generation, operating independently of a commercial grid. Advanced power control techniques were implemented to regulate active-reactive power and dump loads, enabling multiple sources to connect to a single line and allowing flexible system expansion. Such systems are particularly suited for isolated islands and rural areas lacking grid access, contributing to sustainable energy development.

Overall, the literature indicates that hybrid renewable systems integrated with intelligent ANN-based controllers provide a viable approach for achieving efficient, reliable, and sustainable power generation. The combination of wind, solar, energy storage, and advanced control not only reduces reliance on fossil fuels but also ensures stable power delivery in remote, islanded, or grid-connected microgrids. Despite significant progress, ongoing research is focused on improving control strategies, optimizing system architecture, and enhancing the predictive capabilities of ANN controllers to further improve the performance and reliability of hybrid converterless microgrids.

1.3 Problem Formulation

The integration of hybrid renewable energy sources, such as wind turbines and solar PV systems, into the AC utility grid presents a significant challenge due to their intermittent and variable nature. In a converterless microgrid, the direct coupling of DC renewable sources to the grid further complicates voltage and frequency regulation, resulting in potential power quality issues such as voltage sag,

frequency deviations, and harmonic distortions. The Battery Energy Storage System (BESS) and fuel cells can help mitigate these fluctuations, but their operation is constrained by charging/discharging limits, state-of-charge requirements, and response time.

Traditional control methods such as PI or PID controllers are limited in handling the nonlinearities, dynamic interactions, and uncertainties inherent in multi-source hybrid microgrids. Moreover, in minimized-converter architectures, the coupling between the DC bus and PV system requires advanced control strategies that can adapt in real time to variations in renewable generation and load demand. This creates a complex control problem: ensuring stable, efficient, and high-quality power exchange between the hybrid microgrid and the grid, while simultaneously managing bidirectional power flow, maximum power point tracking (MPPT) for PV and wind, and energy storage coordination.

The primary objective is therefore to design an Artificial Neural Network (ANN)-based controller capable of:

- 1. Predicting and compensating for the intermittency of PV and wind sources.
- 2. Coordinating power flow from multiple DC and AC sources to maintain grid stability.
- 3. Managing BESS and fuel cell operation to provide continuous, high-quality power.
- 4. Operating effectively in a converterless microgrid topology, minimizing reliance on conventional converters while improving power quality.

In summary, the problem is to develop an intelligent, adaptive control strategy that can ensure reliable, efficient, and stable operation of a hybrid microgrid with minimal converter architecture, enabling seamless integration with the utility grid while addressing the inherent challenges of renewable energy intermittency, load variability, and limited energy storage capabilities.

1.4 Objectives of project:

The primary objectives of this project focus on the design, simulation, and control of a hybrid renewable energy system to ensure efficient, reliable, and high-quality power delivery. These objectives are:

1. Maximize Power Extraction from Renewable Sources Develop a simulation model of the

hybrid system and implement Maximum Power Point Tracking (MPPT) techniques for solar PV and wind energy to operate at optimal power levels.

- Autonomous Hybrid System Simulation Construct a simulation model of a Solar-Wind-Fuel Hybrid Energy System (SWHES) to analyze performance under varying environmental and load conditions.
- 3. Integration and Control of Multi-Source Microgrid: Implement an ANN-based controller to manage bidirectional power flow, coordinate BESS and fuel cell operation, and enable seamless grid integration in a converterless microgrid architecture. Comprehensive Simulation and Testingof the simulation model to evaluate system stability, power quality, and energy management strategies under realistic operating conditions.

DESIGN AND ANALYSIS OF ANN-BASED INTELLIGENT CONTROLLER

III. ARTIFICIAL NEURAL NETWORK

3.1 Introduction

An Artificial Neural Network (ANN) Controller is an intelligent control system that uses artificial neural networks to model, learn, and control complex and nonlinear dynamic systems. Unlike conventional controllers such as PID, which require a precise mathematical model, ANN controllers can learn the system behavior from data through training. ANNs are inspired by the biological structure of the human

brain, consisting of interconnected processing elements called neurons. These neurons work together to process information and make decisions.

3.2 Fundamentals and OperatingPrinciples of ANN Controller

The basic idea behind an ANN controller is to use a trained neural network to map the relationship between:

- Input variables (such as error, change in error, etc.)
- Output control signals (such as voltage, current, speed, or duty cycle)

Once trained, the ANN can generate control actions automatically to achieve the desired output, even under changing or uncertain conditions.

3.3Structure and Architecture of ANN Controller

An Artificial Neural Network (ANN) controller typically consists of three main layers: the Input Layer, Hidden Layer(s), and Output Layer. Each of these layers plays a vital role in processing information and generating control signals. The Input Layer accepts input signals from the system, such as the error signal (e = reference - actual output) and the rate of change of error (Δe). These signals represent the system's deviation from desired performance and help the controller make corrective adjustments. The Hidden Layer(s) contain several neurons that process input data using activation functions, performing nonlinear mapping from input to output. Common activation functions include the Sigmoid, Tanh, and ReLU functions, which allow the network to handle complex, nonlinear relationships in control systems. The Output Layer produces

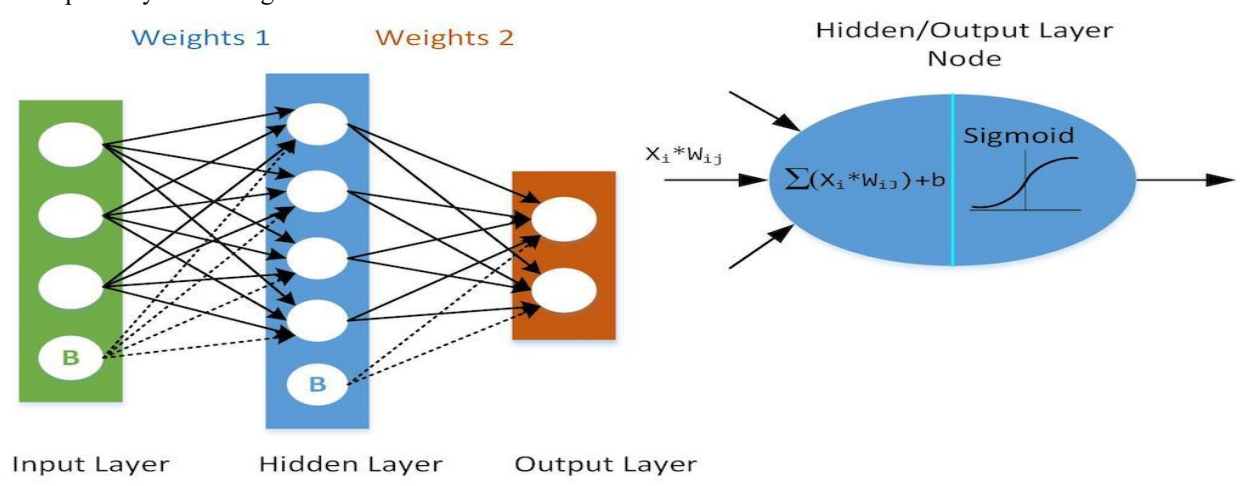


Figure 3.1: Basic architecture of a neural network.

The final control signal that drives the system, such as the duty cycle in a DC-DC converter or control voltage in a motor drive.

In a typical neural network structure, biases are included as additional neurons in both the input and hidden layers. These biases have a fixed, non-zero value (often 1) and are multiplied by specific weight coefficients before being added to the weighted input sums. Figure 3.1 illustrates the architecture of a two-layer neural network. In the hidden layer, each neuron first sums all incoming weighted signals and

then passes the result through an activation function, also known as a limiter. The Sigmoid function is a commonly used limiter and is defined as:

$$S(x) = \frac{1}{1 + e^{-x}} \dots (3.1)$$

This function is preferred because it can be easily differentiated, a property essential for training the network. Similar neuron structures exist in the output layer, where the inputs are signals from the hidden layer.

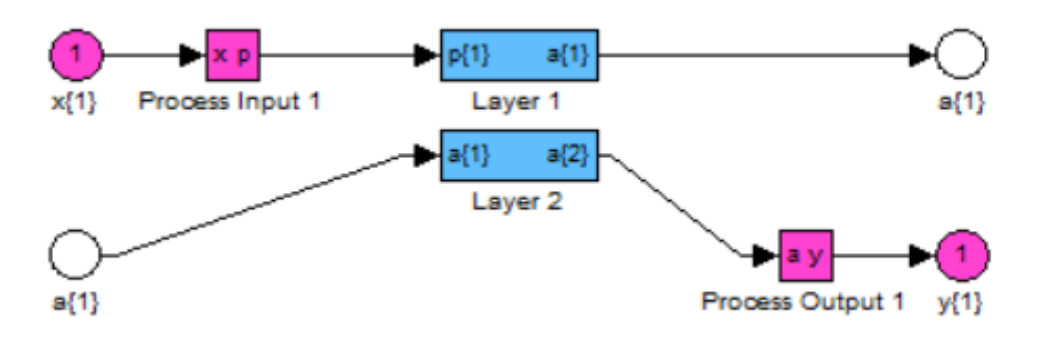


Figure 3.2: Layers of Artificial neural network.

The accuracy of an ANN depends on the weight coefficients, which determine how strongly each input affects the output. Proper tuning of these weights allows the network to approximate complex mappings between input and output data, represented mathematically as y = Wx + b. While a suitable mapping can be found without using bias terms, including them generally improves accuracy. Adding more hidden layers allows the network to perform nonlinear mappings, enhancing flexibility and precision. The process of refining these weight coefficients is known as training the neural network. Training involves two main steps: feedforward and backpropagation. During the feedforward phase, the predicted output (\hat{y}) is calculated as:

$$\hat{y} = \phi(W_2 \phi(W_1 x + b_1) + b_2) \dots (3.2)$$

The difference between the predicted output (\hat{y}) and the desired output (y) is measured using a loss function, which quantifies the network's error. A simple and widely used loss function is the sum-of-squares error. The goal of training is to minimize this loss by adjusting the weights, a process that requires

finding the global minimum of the loss function. Since the loss function depends indirectly on the weights, the chain rule is applied to calculate the partial derivatives with respect to each weight:

$$\frac{\partial Loss(y,\hat{y})}{\partial W} = 2(y - \hat{y}) \cdot \phi' \cdot x$$

This forms the basis of the backpropagation algorithm, where errors are propagated backward from the output layer through the hidden layer to update weights. The derivative of the Sigmoid function used in this process is:

$$\phi'(u) = \phi(u)(1 - \phi(u))$$

This simple derivative allows efficient computation during training. The backpropagation process iteratively updates the weights between the layers (W₁, W₂) to minimize error, ultimately enabling the ANN to accurately map inputs to outputs and control the system effectively.

3.5 OperationalWorking of ANN Controller

An Artificial Neural Network (ANN) controller for a smart grid function as an intelligent and adaptive system capable of learning from real-time and historical data to manage power flow, regulate voltage, and detect faults effectively. Acting as a complex, parallel processing unit, it continuously monitors grid parameters such as voltage, current, load demand, and renewable energy generation. This information is processed through multiple interconnected layers, enabling the ANN to ensure stable and efficient grid performance even under fluctuating conditions.

The input layer of the ANN receives real-time data from the smart grid, including voltage and current levels, power demand, and renewable source outputs like solar and wind. Historical grid stability and fault records are also used to enhance learning accuracy. This input data serves as the foundation for the ANN's decision-making process. The hidden layers perform complex mathematical operations using weighted interconnections and activation functions. Each neuron processes the data, identifies non-linear relationships, and extracts patterns essential for optimizing grid performance. During training, the ANN adjusts these connection weights to minimize errors and improve prediction accuracy, effectively "learning" how to respond optimally under different operating conditions.

After processing through the hidden layers, the output layer generates control signals that are sent to grid components such as inverters, switches, and energy storage systems. These control signals perform key functions like adjusting power flow to balance supply and demand, optimizing renewable and conventional energy distribution, maintaining voltage and reactive power stability, managing battery charging and discharging, and detecting as well as mitigating faults such as line-to-ground failures or islanding. Additionally, the ANN coordinates inverter operations to maintain synchronization and ensure high power quality within the grid.

One of the most significant advantages of ANN-based controllers is their real-time control capability, allowing them to make continuous adjustments to grid operations based on changing conditions. Their adaptive learning ability enables them to respond effectively to variations in load and renewable generation, outperforming conventional controllers

like proportional-integral (PI) systems. Furthermore, their predictive capabilities allow early detection of potential instabilities and faults, enabling proactive intervention to prevent system failures. By reducing harmonic distortions, enhancing voltage stability, and improving power quality, ANN controllers play a crucial role in ensuring a cleaner, more efficient, and reliable smart grid.

3.6Advantages of ANN Controller.

ANN (Artificial Neural Network) controllers provide several significant advantages that make them highly effective for modern control and optimization tasks. They are particularly well-suited for 307tilized307 complex, non-linear systems and demonstrate strong adaptive and self-learning capabilities, allowing them to handle system uncertainties and dynamic variations efficiently. One of their key strengths is their ability to generalize from training data, enabling them to make accurate predictions and control decisions even in new or unseen operating conditions. In addition, ANN controllers exhibit fault tolerance, maintaining system functionality even when some components fail, and support parallel processing, which allows them to handle multiple simultaneously and perform complex computations in real time.

A major advantage of ANN controllers is their capability to model complex and non-linear systems. Unlike traditional control approaches that require precise mathematical models, ANNs can learn intricate input—output relationships directly from operational data. This makes them ideal for controlling systems that are difficult to model analytically, such as chemical reactors, rolling mills, and renewable energy systems. Their adaptability and self-learning features enable continuous improvement of control performance based on real-time data, ensuring stable and efficient operation even under varying environmental or load conditions.

Another distinctive benefit of ANN controllers is that they do not require a predefined system model. Instead, they can learn directly from observed input and output data, which simplifies implementation in complex systems where analytical 307tilized307 is challenging. Additionally, their ability to generalize allows them to respond effectively to new scenarios after being trained on representative datasets. Their fault-tolerant nature ensures that the overall control

system remains operational even if individual neurons or components malfunction, and their parallel processing capability enhances computational efficiency. Moreover, ANNs impose no restrictions on input variables, making them flexible and versatile for a wide range of data types and control applications.

3.7Applications of ANN Controller in Power System Artificial Neural Network (ANN) controllers are highly versatile and are applied across a wide range of fields, including process control, optimization, healthcare, power systems, machine vision, agriculture, and adaptive control. They excel at modelling complex, non-linear systems and learning from data, which makes them essential for solving dynamic and data-driven problems. In process control and optimization, ANN controllers are used to model and regulate intricate industrial processes such as anaerobic reactors for methane production and power electronic converters for improving efficiency and minimizing harmonics. In the healthcare sector, ANNs are applied for medical image analysis, disease detection such as cancer, predicting health risks, and developing personalized treatment plans based on patient data.

Virtual personal assistants like Siri, Alexa, and Google Assistant also utilize ANNs to understand and process natural language, allowing them to interpret voice commands and respond intelligently to user requests. In social media and e-commerce, ANN models are used to analyze user behavior, personalize content, recommend products, and deliver targeted advertisements, thereby enhancing user engagement and experience. In power systems, ANN controllers play a vital role in improving the reliability, efficiency, and control of electrical drives and renewable energy systems. Similarly, in machine vision applications, ANNs are used for food safety and quality control, interpreting spectroscopic data to detect the physical and chemical properties of food products.

In agriculture, ANN-based systems are used for optimizing the operation of agricultural machinery such as combine harvesters, particularly for cruise control systems that adjust engine speed and other settings for improved efficiency. Furthermore, in adaptive control systems, ANNs are often combined with traditional control methods like PID controllers

to create intelligent, self-learning systems capable of adapting to changing conditions and maintaining optimal performance. Overall, ANN controllers bridge the gap between classical control theory and modern intelligent systems, enabling advanced automation, precise optimization, and high-performance control across numerous industrial and real-world applications.

SYSTEM MODELING

V. MODELING OF MICROGRID

5.1 Introduction

To power local needs, the proposed setup is a dieselwind-solar PV standalone microgrid connected to a battery storage system. The overall network architecture is depicted in Fig. The following considerations led to the decision to employ a SyRG as the DG and a PMBLDCG for the wind. Both of these generators are brushless, meaning they require less upkeep than their brushed counterparts. In an asynchronous DG, a SyRG is used in place of a traditional synchronous generator; this eliminates the requirement for a speed governor and automatic voltage regulator, but leaves VSC to handle voltage and frequency regulation. A wind turbine provides the power for the PMBLDC generator. Following what is depicted in Figure. The WECS is linked to the VSC's dc connection through a diode rectifier and a boost converter, as shown in 4.1. Due to the trapezoidal shape of the back EMF, PMBLDCG works well for unsupervised rectification. A lowripple torque is generated, and the machine functions smoothly, if the winding currents are also made quasi-squarewave. PMSG lacks this quality because the EMF generated is sinusoidal, leading to a varying torque from the quasi-square wave currents. The PMBLDC machine has a high energy density despite its compact size, making it an excellent choice for pole-mounted installations. In order to transport energy from the dc link of the VSC to the ac side where loads are located, the suggested topology also includes a solar PV system. As was previously said, the battery energy storagedevice is necessary to preserve the power balance and supply reliability. Therefore, a battery bank is set up at the VSC's dc link.

In order to maximise fuel economy and extract as much free energy as possible, an operational strategy is devised to take use of the proposed system topology's multiple sources. Since the DG is the only ac source, the system and load endfrequency are directly tied to the DG's performance. Since the SyRG generator operates at a constant speed, a constant system frequency implies the same. Some claim that diesel engines are less efficient at lower

loads because their fuel consumption remains relatively constant at fixed speeds during operation. Between 80% and 100% of their rated capacity, diesel engines perform efficiently. Here, we build the DG's control strategy so that it operates only within the loading range depicted in Figure 5.1. Since renewable energy sources and a battery energy storage device are already available, there is no need for a DG with a full load rating.

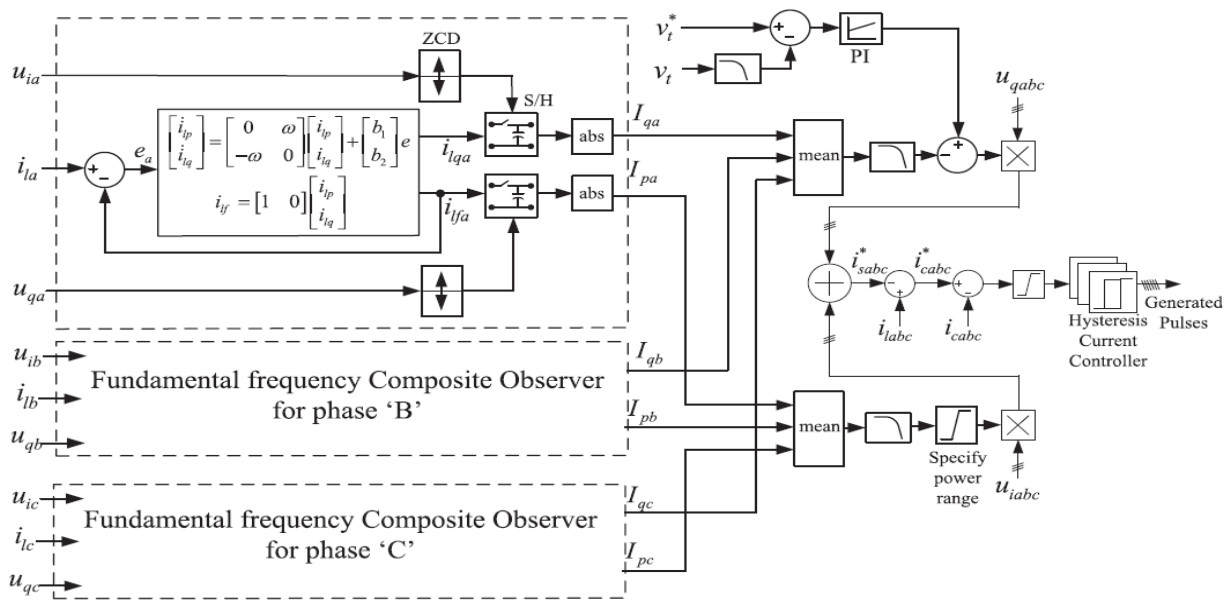


Figure 5.1 VSC's method of control.

The WECS has a PMBLDC generator, a DBR with three phases, and a boost converter. After the DBR, an inductor maintains a nearly constant dc current, which appears as a nearly square ac current waveform, which is useful for the operation of PMBLDCG. Having no requirement for a mechanical sensor for MPPT greatly simplifies the use of the WECS. The Vdc and Idc sensors are not necessary for the MPPT algorithm to function. This maximum power point tracking (MPPT) methodology is identical to the perturb and observe method used in solar PV systems.

5.2. Modeling of Distributed Generation (DG)Units The Fourier series provides a method for dissecting a distorted voltage or current signal into its component dc and sinusoidal signals of varying frequency. Using composite observers, we can estimate all of these frequency components in real time. The fundamental frequency components are all that's

needed for the control algorithm in this system. Here we present the fundamental structure of a composite observer, which generates in-phase and quadraturephase components of the input signal at a certain frequency, allowing us to extract the fundamental frequency component of the load currents. When there are multiple units of a composite observer present, each one has a tendency to extract the harmonic component for which it is tuned. Therefore, the sum of these parts is closer to the true signal. Therefore, the "e" error becomes zero in this form of system. But the proposed method only employs the unit that corresponds to the fundamental frequency, so only the fundamental frequency component is extracted. Load currents are used to estimate their active and reactive power components, as shown in Figure 5.1, where the in-phase component is obtained as the system's output and the quadrature-phase is obtained as the system's internal state. 4.2. It is necessary to have both in-phase and quadrature-phase

© November 2025 | IJIRT | Volume 12 Issue 6 | ISSN: 2349-6002

unitvectors of PCC voltage in order to produce reference source currents. The voltage-frequency controller (VSC) control algorithm is depicted in Figure. The voltage support converter (VSC) keeps the generator's active power output constant, in turn controlling the frequency indirectly.

5.5. Battery Energy Storage System (BESS) modelling and control

Though the study primarily focuses on the hybrid generation system, this section is devoted to elucidating the power flows in the topology and offering suggestions for managing the battery's charge and discharge. Large-scale demonstration of power flow between the various sources is shown in Figure 5.4. Since all other currents and powers are known, it should be straightforward to estimate the battery current and act accordingly. Topology and controls presented allow for independent regulation of battery charge and discharge by independent regulation of each power source and load, as depicted in Figure 5.4. A current sensor can detect the current flowing through the battery in the event that precise monitoring of the charge discharge is required. Battery voltage readings are already being taken, so they can be 310tilized to calculate state of charge and other discharge-control parameters.

Power Flow and Available Controls in the Hybrid Generation System

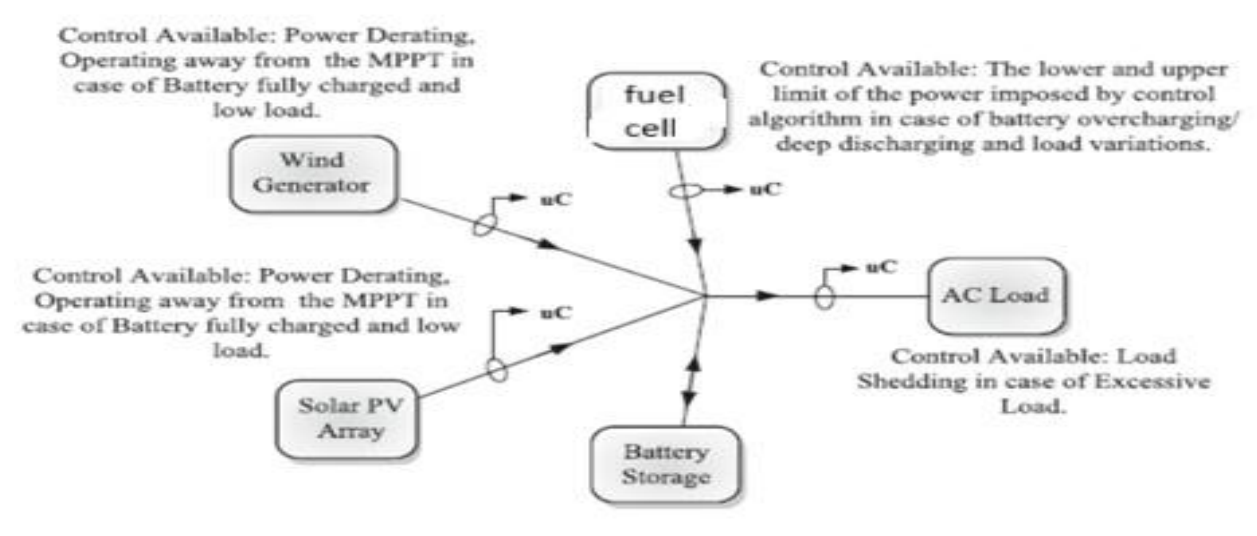


Figure 5.4 Flow of power and system controls

SIMULATION RESULTS

VI. SIMULATION

6.1 Configuration and Operation of a DC-Coupled Hybrid Microgrid

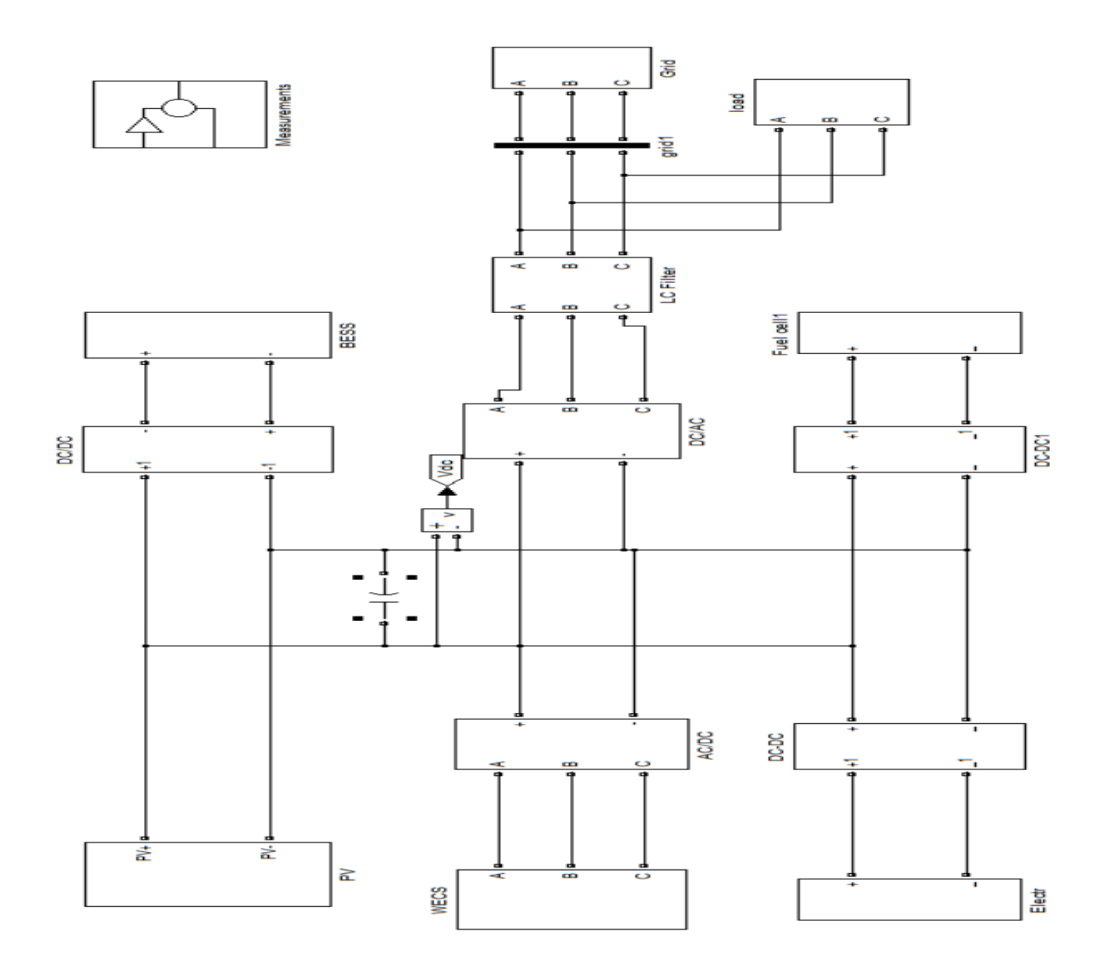


Figure 6.1 Simulation Diagram of Hybrid PV-Wind-Fuel Cell Microgrid System with Grid Integration
The Figure 6.1 illustrates a typical configuration of a DC-coupled hybrid microgrid system. This setup is designed to integrate multiple energy sources, condition and regulate their outputs on a shared DC bus, and deliver high-quality AC power to both local loads and the main utility grid. The architecture ensures optimal power management, seamless source coordination, and efficient energy utilization across renewable and auxiliary units.

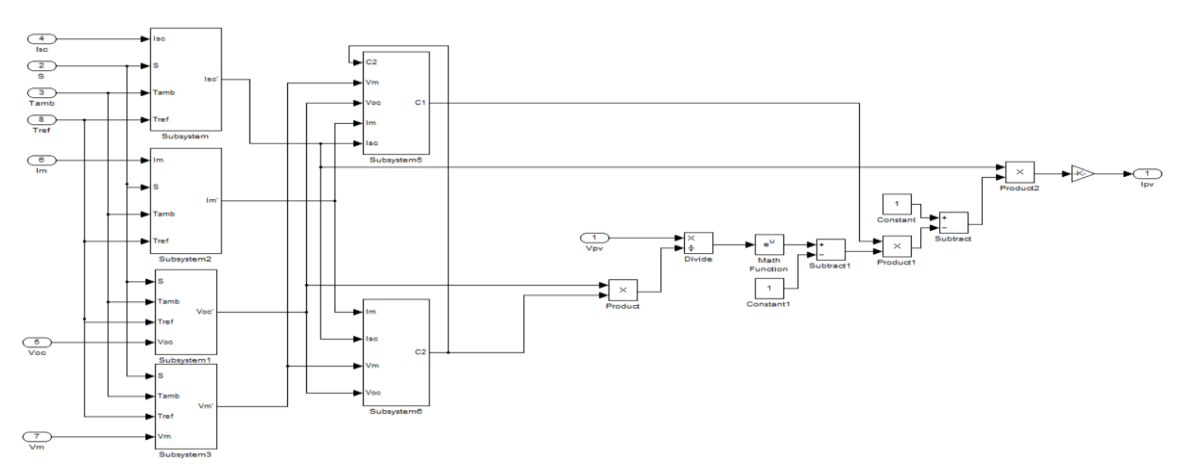


Figure 6.2 Simulink Model of a Photovoltaic (PV) Cell/Module

The renewable energy sources in the system primarily include a Photovoltaic (PV) array and a Wind Energy Conversion System (WECS). The PV array generates direct current (DC) power, which is interfaced to the main DC bus through a dedicated DC/DC converter.

This converter regulates the PV output voltage and current to maintain maximum power point tracking (MPPT) and ensure stable integration with the DC bus. The WECS, on the other hand, produces alternating current (AC) power through a wind turbine generator. This AC output is rectified by an AC/DC converter (rectifier) before being connected to the DC bus. Together, these renewable sources contribute to the primary energy generation capacity of the hybrid microgrid.

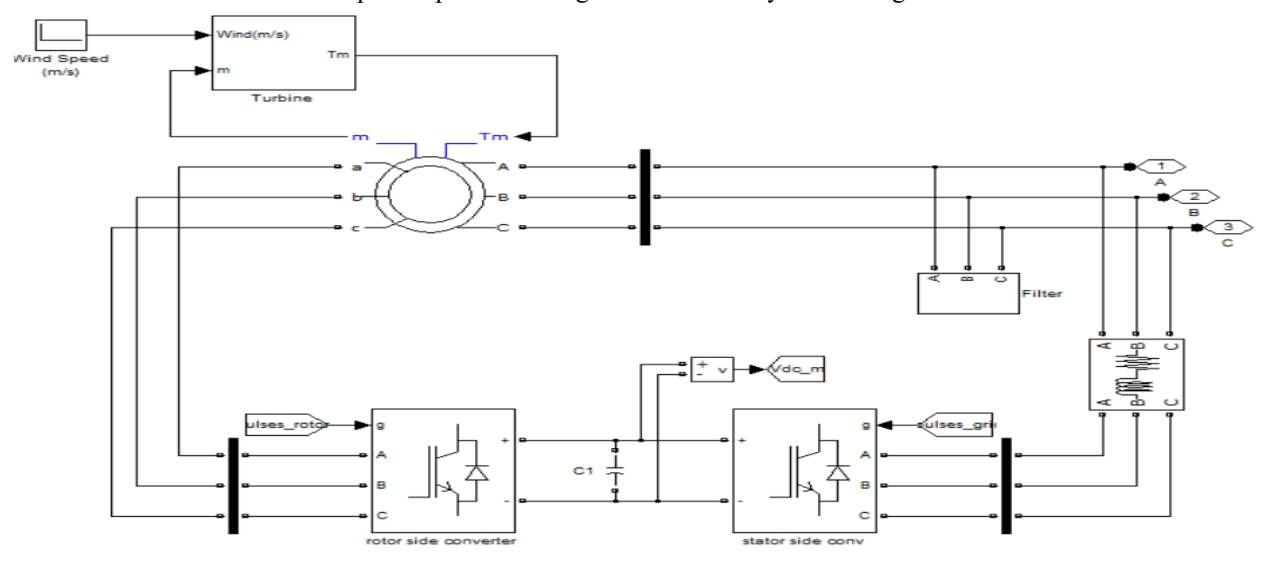


Figure 6.3 Simulink Model of a Doubly Fed Induction Generator (DFIG) Wind Energy System

The system also includes energy storage and auxiliary power components that enhance reliability and stability. A Battery Energy Storage System (BESS) is connected to the DC bus through a bidirectional DC/DC converter, enabling both charging and discharging operations. The BESS supports load balancing, power quality improvement, and grid support during transient conditions. In addition, a Fuel Cell (FC) unit is included as a clean DC power source, interfaced to the DC bus via a converter (labeled DC–DC1). Complementing the fuel cell is an Electrolyzer block,typically labeled "Electr" or

"Electrolysis," which converts surplus electrical energy into hydrogen through the electrolysis process. This stored hydrogen can later be utilized by the fuel cell to regenerate electrical power, effectively closing the power-to-gas-to-power cycle and providing an efficient auxiliary energy pathway.

At the heart of this architecture lies the common DC bus, denoted as V_{dc} . This bus serves as the central power aggregation and regulation point where all source and storage units are interconnected. A capacitor bank (C) is installed across the DC link

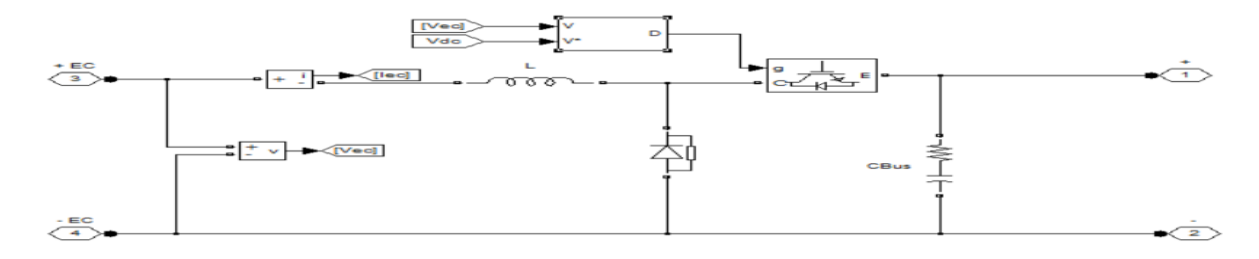


Figure 6.4Controlled DC-DC Buck Converter Circuit Simulation

to smooth voltage fluctuations, filter noise, and stabilize the DC voltage under dynamic load variations. From this DC bus, the power is fed into a DC/AC inverter, which performs the critical task of converting the regulated DC voltage into a high-quality three-phase AC signal suitable for supply to AC loads and grid interconnection.

The output and grid interface section ensures that the generated AC power meets grid standards and load requirements. The inverter output passes through an LC filter, composed of inductors and capacitors, which attenuates switching harmonics and refines the

AC waveform, ensuring compliance with grid power quality norms. The filtered AC output is then delivered to the Point of Common Coupling (PCC), labeled as grid1, which represents the interface between themicrogrid and the utility network. From this point, the system can either export power to the grid when local generation exceeds demand or import power when renewable sources are insufficient. The local load, represented as a three-phase AC load, receives stable and conditioned power from the same PCC, ensuring uninterrupted operation of connected homes, industries, or community systems.

6.3 PV System Input Irradiance Profile Over Time

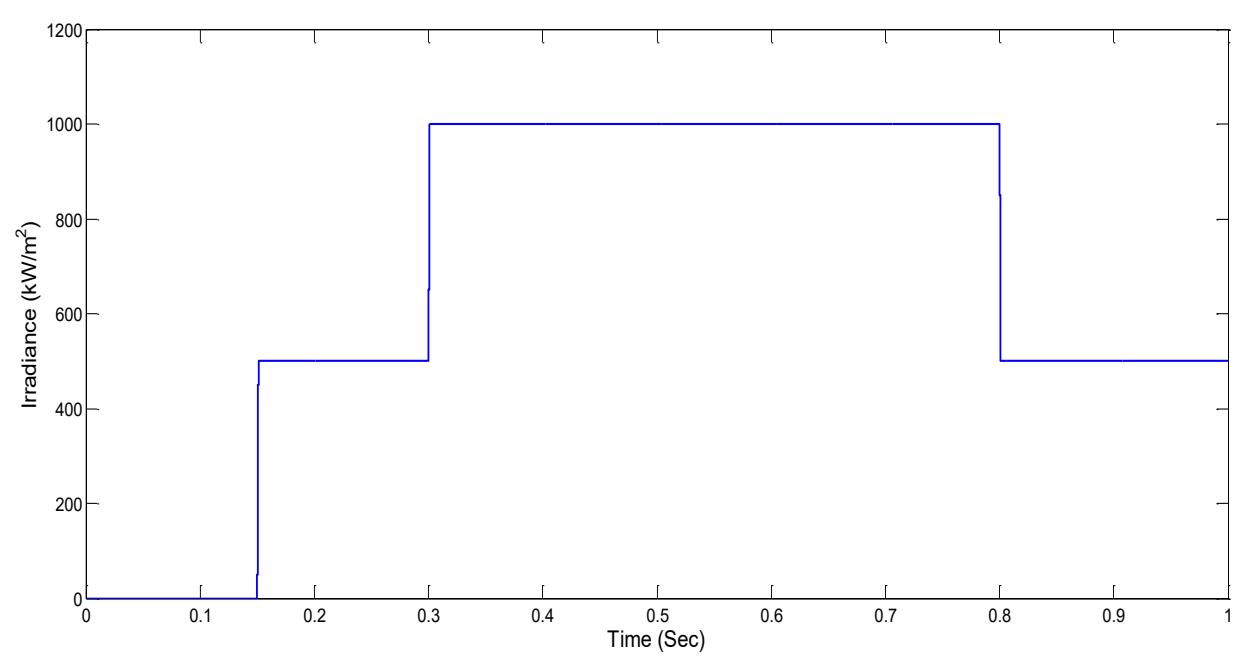


Figure 6.8 PV system input irradiance

This figure 6.8 represents the input solar irradiance applied to a photovoltaic (PV) system over time, typically as part of a simulation in a hybrid renewable energy system or DC microgrid. The irradiance pattern defines how much solar power is incident on the PV panels during the simulation, directly affecting the output power of the PV array.X-Axis (Time in seconds) The simulation time runs from 0 to 1 second.Each segment represents a different irradiance level applied at a specific time interval. Y-Axis (Irradiance in W/m²) Irradiance values range from 0 to 1200 W/m².This represents the intensity of sunlight falling on the PV array surface.A higher irradiance value means more sunlight and, therefore,

higher PV output power. Initial Condition $(0-0.1\,\mathrm{sec})$ Irradiance = 0 W/m²At the start, the PV array receives no sunlight, simulating nighttime or a noinput condition. Hence, the PV system produces no electrical power during this period. First Step Change ($\approx 0.1-0.3\,\mathrm{sec}$) Irradiance increases to around 400 W/m² at 0.1 sec and then to 1000 W/m² at 0.3 sec. These two step increases mimic morning solar intensity rise as the sun begins to shine. The PV system's output voltage and current will increase proportionally with irradiance, as per the PV cell characteristic equation where I_{ph} depends directly on irradiance.

6.4 Current and Power Output vs. Voltage for the PV Array

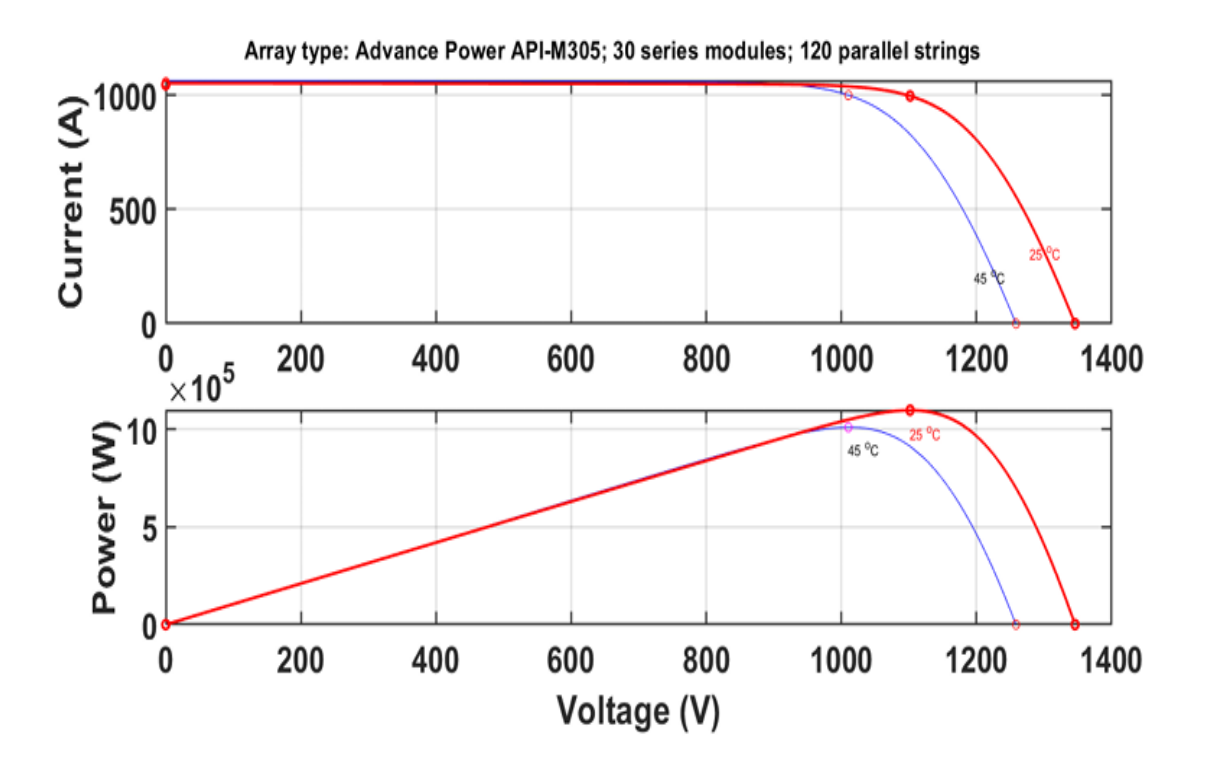


Figure 6.9 I-V (Current vs. Voltage) and P-V (Power vs. Voltage) characteristics of a photovoltaic (PV)

The given diagram illustrates the I–V (Current vs. Voltage) and P–V (Power vs. Voltage) characteristics of a photovoltaic (PV) array, specifically for the Advance Power API-M305 module type. The array consists of 30 modules connected in series and 120 parallel strings. There are two plots shown in the figure: the top plot represents the Current (A) versus Voltage (V) characteristic, and the bottom plot represents the Power (W) versus Voltage (V) characteristic. Both curves are plotted for two different operating temperatures, 25°C (red curve) and 45°C (blue curve), to study the effect of temperature on array performance.

In the I–V curve, the current remains nearly constant as the voltage increases up to a certain point known as the knee point or maximum power point (MPP). Beyond this point, the current drops sharply to zero. As the temperature increases, the open-circuit voltage (Voc) decreases, while the short-circuit current (Isc) increases slightly. This indicates that at higher temperatures, the voltage output of the PV array decreases, and although the current increases

marginally, the overall power generation capability is reduced.

In the P–V curve, the power output rises with voltage until it reaches the maximum power point (Pmax), after which it declines rapidly. At 25°C, the maximum power is higher and occurs at a higher voltage, whereas at 45°C, the maximum power decreases and occurs at a lower voltage. This demonstrates that the efficiency of a PV module decreases with increasing temperature.

6.5 Output Power Characteristics of PV Array

Figure 6.10 illustrates how the power output from a solar photovoltaic (PV) array varies with time under changing solar irradiance or environmental conditions. The x-axis represents time in seconds, and the y-axis represents PV power in megawatts (MW × 10⁵). The curve shows distinct step changes in PV output, indicating how the PV system responds dynamically to sudden variations in sunlight intensity or load demand. During the initial period from 0 to 0.2 seconds, the PV power remains at zero, signifying no solar generation, which

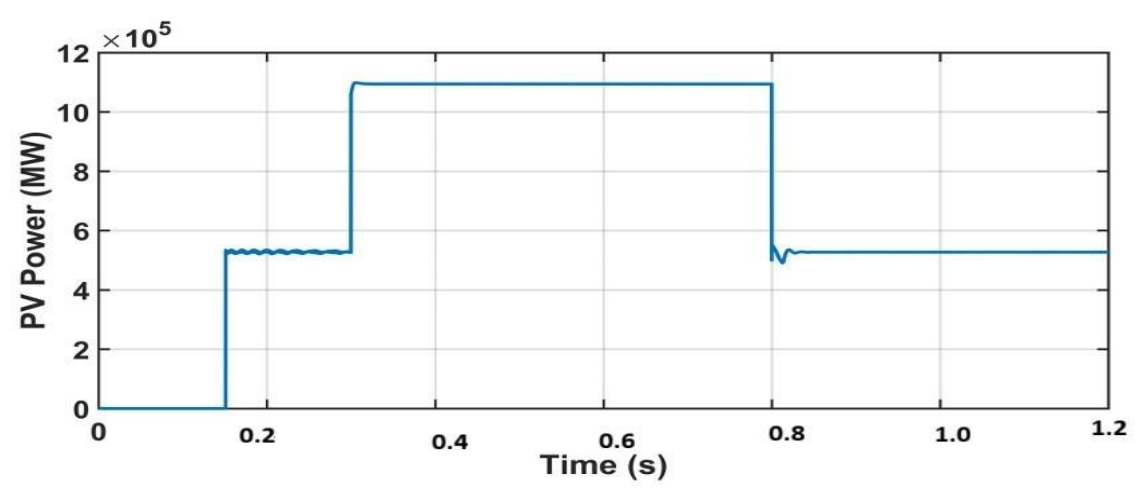


Figure 6.10PV Power vs. Time Characteristics may occur before sunlight exposure or during system startup. Between 0.2 and 0.3 seconds, the power rises sharply to about 5 × 10⁵ MW, representing an increase in solar irradiance or system activation. From 0.3 to 0.8 seconds, the PV output maintains a steady high level of approximately 10 × 10⁵ MW, corresponding to maximum power generation under full sunlight conditions. Finally, from 0.8 to 1.2 seconds, the power drops back to around 5×10^5 MW, which may be due to partial shading, a decrease in irradiance, or a change in load. Overall, this figure represents the dynamic response of PV power generation to varying solar irradiance environmental conditions, demonstrating the ability of the PV system to quickly adjust its output and maintain stability under transient changes.

6.6 DC-Link Voltage (Vdc) Tracking its Step-Changed Reference (Vdcref)

This figure 6.6 shows the DC-link voltage dynamic response in a DFIG-based wind energy system (or any grid-connected converter system). The x-axis represents Time (sec) and the y-axis represents DClink Voltage (V). Two signals are plotted blue line (Vdc ref) Reference DC-link voltage (desired voltage set by the control system) and red line (Vdc) Actual DC-link voltage measured during operation. The Vdc controller (part of the Grid Side Converter control loop) is performing voltage regulation effectively. The transient overshoot is quickly damped, showing that the ANN or PI controller is well-tuned. The tracking of Vdc ref after both step increases and decreases demonstrates: Fast dynamic response, Strong disturbance rejection, and accurate steadystate control. Maintaining a stable DC-link voltage ensures

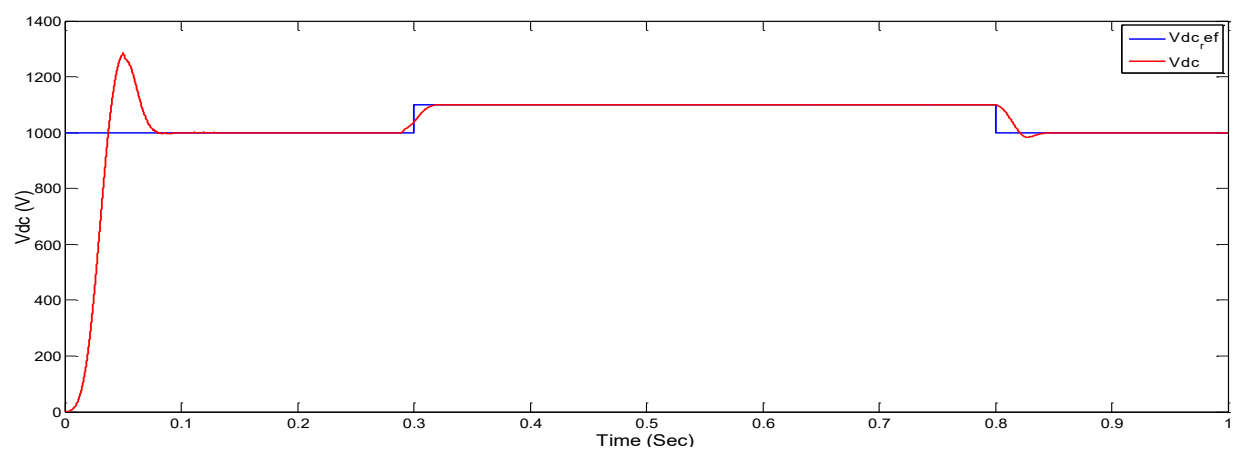


Figure 6.11 DC reference voltage and measured

continuous and bidirectional power flow between generator and grid with minimum ripple. This figure illustrates the excellent DC-link voltage control performance of the converter system. The voltage closely follows its reference under both steady and transient conditions, ensuring smooth energy transfer between the machine and the grid. The small overshoots and quick settling confirm the controller's robustness, fast. Such behavior is essential in renewable energy systems (like DFIG wind systems) to maintain power quality, voltage stability, and reliable grid interfacing.

6.7 Battery Power Response to System Load/Irradiance Changes

Power flow management under varying conditions. The system's control strategy, enabled by the ANN, effectively manages fluctuations in power supply and demand to maintain stability. Handling excess power (charging): When excess generation causes the DC bus voltage to rise, the ANN controller commands the converter to switch to buck mode, absorbing energy and charging the battery. This is represented by the negative power region (0.3–0.8 sec), which relieves stress on the DC bus. Handling power demand (discharging): The system handles load increases or generation drops by discharging the battery. This is implied in the final phase (0.8–1.0 sec) as the

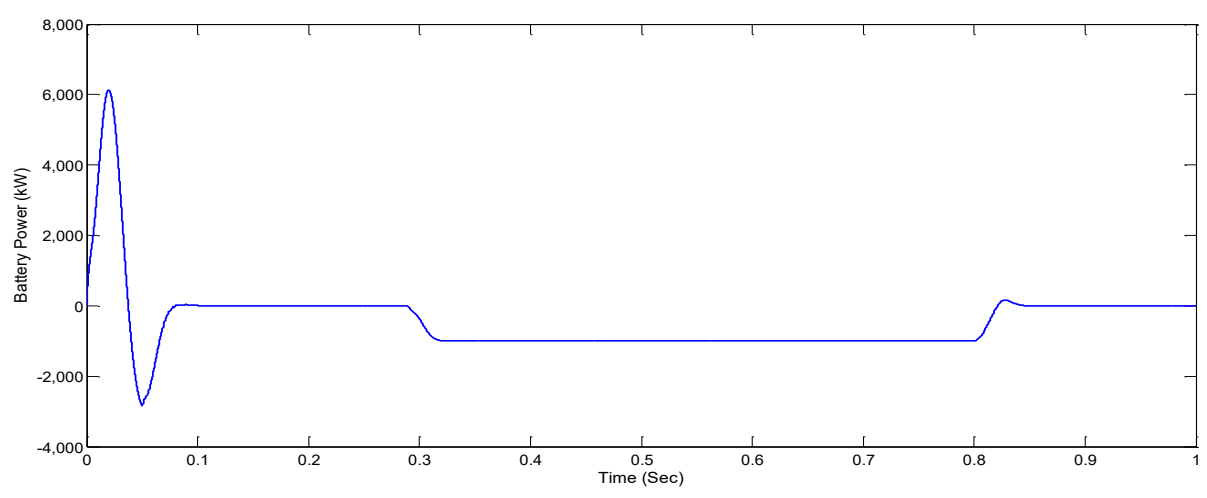


Figure 6.12 Battery Power

power moves toward zero or slightly positive, indicating the battery is ready to supply power if needed. Maintaining DC bus voltage stability: The core function of the BESS is to act as a buffer. By absorbing excess power and injecting power during deficits, the battery system helps to regulate the DC bus voltage, keeping it within a stable operating range. The plot's smooth and stable power control demonstrates the ANN's success in achieving this.

X-Axis (Time in seconds) The simulation runs from 0 to 1 second. This time interval captures both transient and steady-state performance of the battery. Y-Axis (Battery Power in kW) The power value ranges approximately from -4000 to +8000 kW. Positive power represents battery is discharging (supplying power to the system). Negative power represents battery is charging (absorbing power from the DC bus). Initial Transient (0 – 0.1 sec) at the very

start, there are sharp oscillations between +8000 kW and -3000 kW. This represents the dynamic transient response of the system when it first begins operation. Causes of this transient are sudden connection of the battery system to the DC bus.Initial imbalance between reference voltage/current and conditions, Controller (ANN) adjusting duty cycle of the DC-DC converter to stabilize power flowand The Artificial Neural Network (ANN) controller works to quickly suppress these oscillations, stabilizing the system. First Steady-State Region ($\approx 0.1 - 0.3 \text{ sec}$) the power settles close to 0 kW (a nearly flat line). This means the battery neither charges nor discharges significantly. The DC bus voltage is stable, and other sources (like PV or grid) are managing the load. In Second Operating Phase ($\approx 0.3 - 0.8 \text{ sec}$) around 0.3 sec, the power drops to about -2000 kW.This negative region indicates the battery is charging. It happens typically when the DC bus voltage exceeds its reference (excess generation). ANN controller signals the DC-DC converter to absorb energy from the bus between 0.3 and 0.8 sec, the battery maintains this charging mode steadily, showing effective control by the ANN. Final Phase ($\approx 0.8-1~\text{sec}$) Around 0.8 sec, the power briefly moves up towards 0 or slightly positive. This implies The battery transitions back toward discharge mode or becomes idle. It responds to a load increase or generation drop. The smooth transitions again reflect fast adaptation and robust performance of the ANN-controlled converter.

Figure 6.12 Battery Power demonstrates that The battery responds dynamically to system changes. The ANN controller ensures rapid stabilization and accurate power control. The system transitions smoothly between charging and discharging modes, indicating effective coordination between the battery,

DC-DC converter, and the overall hybrid energy system.

6.8 Transient and Steady-State Response of Stator Active and Reactive Power

This figure 6.8 Stator Active and Reactive Power shows the dynamic performance of the stator (likely from an induction generator or motor in a renewable energy system, such as a wind turbine or hybrid DC microgrid) during the simulation period. It depicts how both active power (P) and reactive power (Q) vary with time under control of the associated converter and ANN controller. The figure consists of two subplots Top plot is Stator Active Power (W) and Bottom plot: Stator Reactive Power (VAR) both are plotted as a function of time (seconds) from 0 to 1 second. The curve rises sharply from 0 W at t = 0 to around 6×10^5 W (600 kW) after the initial rise (within ~0.08 s), it rapidly settles to a nearly constant small value close to zero for the rest of the simulation (0.1 - 1 s).

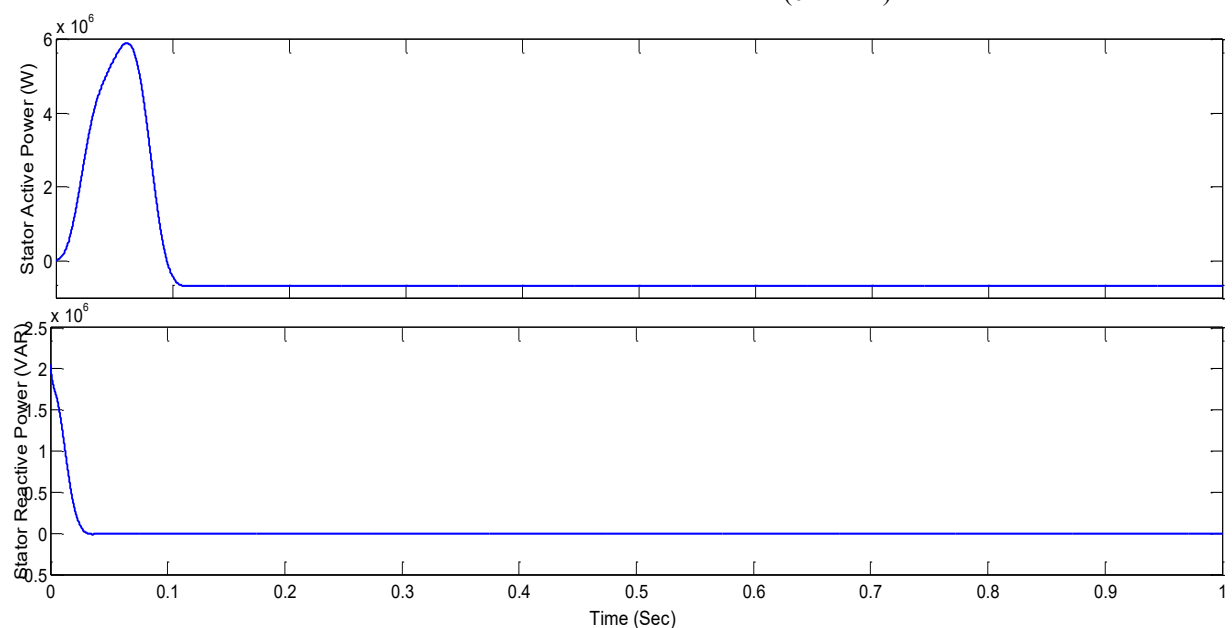


Figure 6.13 Stator Active and Reactive Power

and current to balance power exchange. The stator active power flow becomes minimal once steady DC bus voltage is achieved, meaning the generator is operating efficiently with minimal losses or is idling under no-load condition. The initial peak indicates dynamic response capability. The flat steady portion shows that active power control is well-damped, ensuring stability. A well-designed controller should

show exactly this kind of quick settling with no sustained oscillations.

Stator Reactive Power starts high, near 2×10^5 VAR (200 kVAR) at t = 0. It rapidly decays to zero by around 0.05–0.08 s and then remains flat at zero for the rest of the simulation. Reactive power is associated with the magnetizing component of current in AC machines. The high initial reactive

power is required to build up the magnetic field in the stator windings when the system is first energized. Once the magnetic field stabilizes, reactive power demand drops.

In a hybrid renewable system, this figure likely corresponds to the generator or motor stator connected through a DC-AC converter (inverter) controlled by an Artificial Neural Network (ANN). During the start-up phase, the ANN controller ensures smooth transient performance by minimizing oscillations in both active and reactive power. The fast decay of both P and Q indicates High control

accuracy, reduced electromagnetic torque ripples, andStable coupling between the stator and DC bus. Thus, the figure confirms the dynamic stability and fast convergence of the machine's electrical parameters under ANN control. Both active and reactive powers exhibit short-lived peaks due to initial magnetization. The ANN controller ensures rapid damping and zero steady-state error. The system achieves steady-state operation within 0.1 seconds, confirming the robustness and fast response of the control strategy used.

6.9 Transient and Steady-State Response of Rotor Active and Reactive Power

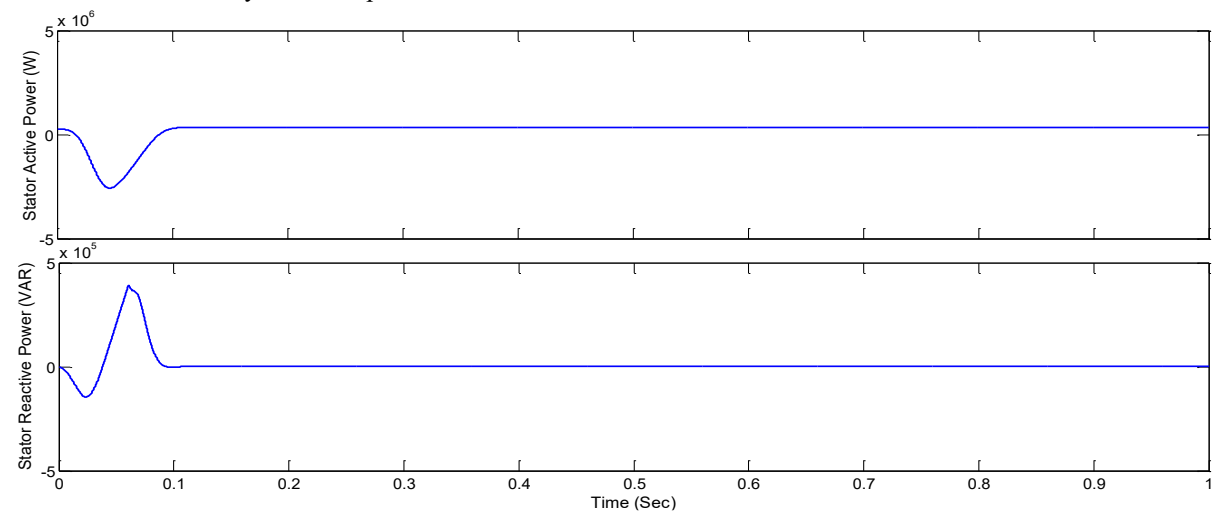


Figure 6.14 Rotor Active and Reactive Power

This figure 6.14 Rotor Active and Reactive Power — shows the dynamic performance of the rotor (most likely of a Doubly Fed Induction Generator (DFIG) or Induction Machine) under varying conditions controlled by a power electronic converter, typically with an ANN (Artificial Neural Network) controller. It represents how both rotor active power (P) and rotor reactive power (Q) evolve over time during the system's transient and steady-state operation. The figure 6.9 contains two subplots Top Plot: Rotor Active Power (W)Bottom Plot: Rotor Reactive Power (VAR)The x-axis for both plots is Time (seconds), running from 0 to 1 second.

The rotor active power starts with a small oscillation around 0 W at the beginning (0–0.05 s). Then it rises positively and settles at a constant value near 5×10^5 W (500 kW) by approximately 0.1 seconds. After this transient, the power remains steady until the end of the simulation. The rotor active power represents the

real electrical power either generated or absorbed by the rotor circuit. The initial oscillation corresponds to sudden connection of the rotor to the converter and establishment of electromagnetic coupling between rotor and stator fields. Inrush current due to the difference between mechanical and electrical rotor speeds at startup. The settling region shows that the ANN-based control effectively damps out transients and stabilizes power flow. Once steady state is reached the rotor supplies active power to the grid or DC bus (positive direction) if operating as a generator. The stabilized value (~500 kW) indicates effective energy conversion and minimal losses.

Figure 6.14 Rotor Active and Reactive Power illustrates the dynamic performance and steady-state stability of the rotor circuit in a controlled generator or motor system.Both active and reactive power exhibit small, short-lived oscillations during system startup.The active power stabilizes rapidly, indicating

© November 2025 | IJIRT | Volume 12 Issue 6 | ISSN: 2349-6002

efficient real power transfer. The reactive power converges to zero, confirming effective power factor correction and magnetic flux stabilization. The ANN controller provides robust damping and precise control, minimizing overshoot and settling time.

Figure 6.14 clearly demonstrates that the rotor circuit, controlled via ANN and converter, achieves a fast transient response, stable steady-state operation, and excellent power quality with negligible reactive power flow. This reflects optimized control coordination between rotor, stator, and the converter interface in a hybrid energy conversion system.

6.10 Grid-Side Converter Active Power Response to System Operating Condition Changes

The figure 6.10 plots the Grid Side Converter (GSC) Active Power (in watts) on the y-axis against Time (in seconds) on the x-axis. The time range is from 0 to 1 second, and the active power varies approximately between -1.5×10^6 W and $+1.2 \times 10^6$ W.

This figure 6.10 represents the active power exchange between the Grid Side Converter (GSC) and the utility grid in a Doubly Fed Induction Generator (DFIG)-based Wind Energy Conversion System (WECS) or in a similar hybrid system where a grid-connected converter controls the power flow. Understanding Active Power behaviour initial Period $(0-0.1~{\rm sec})$: Transient

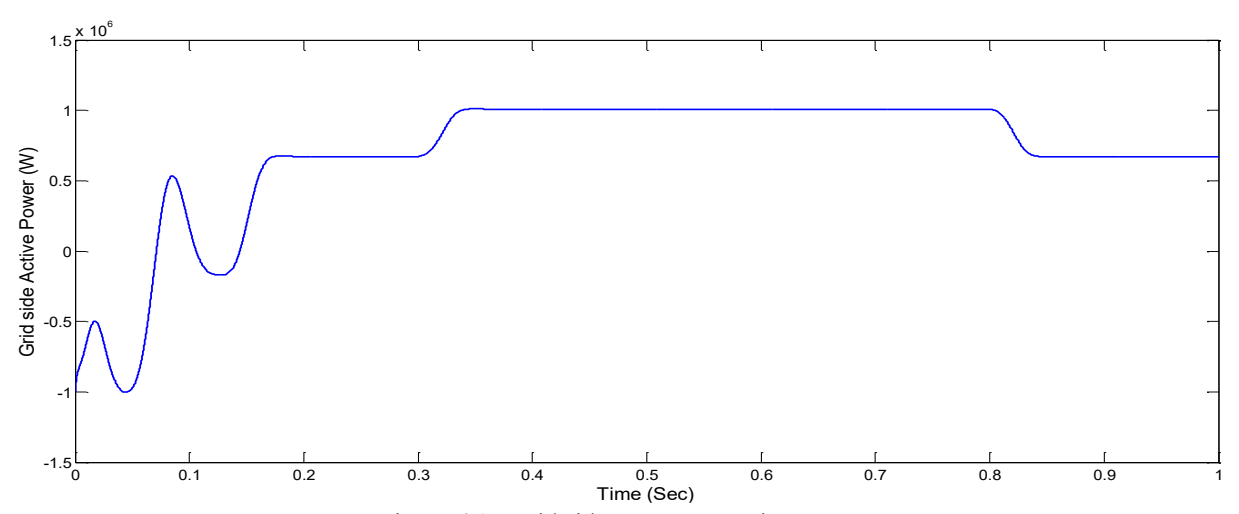


Figure 6.15 Grid side converter Active Power

ResponseAt the start (0-0.1 sec), the waveform shows oscillations and negative power peaks up to −1.2 × 10⁶ W.This indicates transient conditions due to system startup or a sudden change in grid or wind conditions. Negative active power means converter is absorbing power from the grid, which could occur when the DC link capacitor charges up or when the control loop stabilizes. Transition Period (0.1 - 0.3 sec): System StabilizationAfter 0.1 sec, the oscillations gradually reduce. Around 0.2 sec, the power becomes positive and starts to stabilize near 0.6×10^6 W.This shows that the GSC control loop is stabilizing the DC link voltage and synchronizing with the grid frequency. The converter now exports active power to the grid, meaning the DFIG is generating electricity. Steady-State Region (0.3 - 0.8)sec): Constant Power DeliveryBetween 0.3 and 0.8 sec, the active power stabilizes at around 1×10^6 W

(1 MW). This steady output signifies normal grid-connected operation under stable wind or load conditions. During this period, the GSC regulates the DC-link voltage and ensures constant power delivery to the grid. The constant output reflects that the rotor side converter and grid side converter are working in coordination maintaining power balance between rotor and grid sides. End Period (0.8 – 1 sec): Load or Wind Variation after 0.8 sec, there is a slight drop in active power to around 0.6×10^6 W. This change might correspond to A decrease in wind speed, A change in grid demand, or A control action (e.g., reference power reduction). Despite the drop, the waveform remains smooth, showing that the system remains stable and well-controlled.

The Grid Side Converter Active Power plot shows how the converter transitions from transient to steady operation.It successfully stabilizes the DC-link voltage and exports constant active power to the grid after initial oscillations. The small fluctuations demonstrate the converter's dynamic response and power regulation capability under changing conditions. Overall the GSC ensures smooth and stable power delivery, confirming the effectiveness of the ANN controller used.

6.11 Transient Power Response Comparison of Hybrid and Conventional Systems

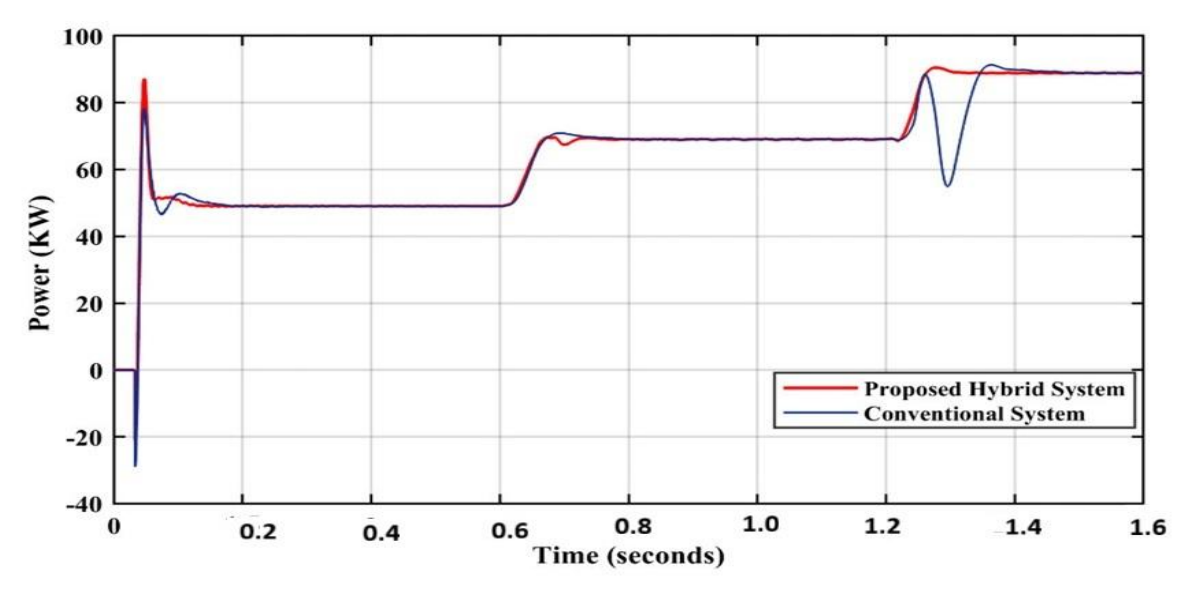


Figure 6.16Power comparison plot (Proposed Hybrid System vs. Conventional System).

This figure 6.16 illustrates a comparative analysis of power output (kW) between a Proposed Hybrid System and a Conventional System over a time duration of 1.6 seconds.

The X-axis represents Time (seconds), and the Y-axis represents Power (kW), ranging approximately from -40 kW to 100 kW. The red curve denotes the Proposed Hybrid System, while the blue curve represents the Conventional System.

At the initial transient period (0–0.1 s), both systems show start-up fluctuations. The Conventional System experiences a negative dip (around –25 kW), whereas the Proposed System exhibits a positive overshoot reaching nearly 90 kW.

During the first steady state (0.2–0.6 s), both systems stabilize at a constant power level. When the first step change (at 0.6 s) occurs, the output power increases to a higher level, and both systems track this step with minimal transient differences.

In the second steady-state region (0.8–1.25 s), both maintain nearly the same power output. However, when the second step change (at 1.25 s) is applied, a clear performance distinction appears. The Conventional System (blue) shows a significant

undershoot (around 55 kW) and a slower settling time. In contrast, the Proposed Hybrid System (red) exhibits only a small overshoot (around 92 kW) and settles faster with minimal oscillations.

VII. CONCLUSION

This study proposes the integration of a Photovoltaic (PV) system and a Wind Energy Conversion System (WECS) for an autonomous micro-grid, with an Artificial Neural Network (ANN)-based control system to optimize performance. The ANN controller is trained to predict the maximum power point (MPP) under varying irradiance, temperature, and wind conditions, enabling efficient operation of a boost converter for PV power extraction. Dual PI loops manage the DC bus voltage and battery charging, while the ANN dynamically adjusts control parameters to respond to fluctuations in renewable generation and load demand.

The battery bank stores excess energy when generation exceeds load and supplies power when renewable output is insufficient. The ANN controller safeguards the batteries against overcharging and over-discharging by monitoring the state of charge (SOC). It disconnects PV and wind sources when SOC exceeds 80% and reconnects them when SOC drops below 75%. If SOC falls below 20%, the inverter and loads are disconnected to prevent damage.

By integrating ANN control, the micro-grid operates autonomously, efficiently managing energy generation, storage, and load demands while adapting to dynamic environmental and load conditions. This approach improves system reliability, stability, and energy utilization compared to conventional PI-based control alone.

The proposed ANN-based control technique effectively minimizes oscillations in the DC-link voltage, improves transient response, and enhances the overall system stability when compared to conventional control methods. The simulation results, obtained using MATLAB/Simulink, clearly validate that the ANN-based hybrid system ensures steady power flow, efficient energy management, reduced converter count, and higher overall efficiency under various environmental and operational conditions. In the previously used control method, the system's power output settled between 8.5 to 12 seconds. However, with the implementation of the ANN controller, the power settles at its final steady-state positive value much faster, reaching stability at around 0.35 seconds. This demonstrates a significant improvement in the dynamic performance and response speed of the system.

VIII. FUTURE SCOPE

The following key future research directions and practical developments can be identified:

- 1. Optimization and Efficiency Enhancement
- 2. System Reliability and Lifespan Improvement
- 3. Real-Time Implementation and Hardware Validation
- 4. Grid Integration and Smart Grid Applications
- 5. Economic and Environmental Analysis
- 6. Scalability and Microgrid Applications

REFERENCES

[1] Bendary, A.F.; Ismail, M.M. Battery charge management for hybrid PV/wind/fuel cell with

- storage battery. Energy Procedia 2019, 162, 107–116. [CrossRef]
- [2] Elavarasan, R.M.; Ghosh, A.; Mallick, T.K.; Krishnamurthy, A.; Saravanan, M. Investigations on performance enhancement measures of the bidirectional converter in PV-wind interconnected microgrid system. Energies 2019, 12, 2672. [CrossRef]
- [3] Muriithi, G.; Chowdhury, S. Optimal energy management of a grid-tied solar PV-battery microgrid: A Reinforcement learning approach. Energies 2021, 14, 2700. [CrossRef]
- [4] Shan, Y.; Hu, J.; Chan, K.W.; Fu, Q.; Guerrero, J.M. Model predictive control of bidirectional DC-DC converters and AC/DC interlinking converters—A new control method for PV-windbattery microgrids. IEEE Trans. Sustain. Energy 2019, 10, 1823–1833. [CrossRef]
- [5] Mahesh, A.; Sandhu, K.S. Hybrid wind/photovoltaic energy system developments: Critical review and findings. Renew. Sustain. Energy Rev. 2015, 52, 1135–1147. [CrossRef]
 - [6] Berardi, U.; Tomassoni, E.; Khaled, K. A smart hybrid energy system grid for energy efficiency in remote areas for the army. Energies 2020, 13, 2279. [CrossRef]
- [7] Murty, V.V.S.N.; Kumar, A. Multi-objective energy management in microgrids with hybrid energy sources and battery energy storage systems. Prot. Control Mod. Power Syst. 2020, 5, 1–20. [CrossRef]
- [8] Alhasnawi, B.N.; Jasim, B.H.; Esteban, M.D. A new robust energy management and control strategy for a hybrid microgrid system based on green energy. Sustainability 2020, 12, 5724. [CrossRef]
- [9] Kumar, G.R.P.; Sattianadan, D.; Vijayakumar, K. A survey on power management strategies of hybrid energy systems in microgrid. Int. J. Electr. Comput. Eng. IJECE 2020, 10, 1667– 1673. [CrossRef]
- [10] Datta, U.; Kalam, A.; Shi, J. Hybrid PV-wind renewable energy sources for microgrid application: An overview. In HybridRenewable Energy Systems in Microgrids; Elsevier BV: Amsterdam, The Netherlands, 2018; pp. 1–22.
- [11] Rehman, S.; Habib, H.U.R.; Wang, S.; Buker, M.S.; Alhems, L.M.; Al Garni, H.Z. Optimal design and model predictive control of

- standalone HRES: A real case study for residential demand side management. IEEE Access 2020, 8, 29767–29814. [CrossRef]
- [12] Fathy, A.; Kaaniche, K.; Alanazi, T.M. Recent approach Based social spider optimizer for optimal sizing of hybrid PV/wind/battery/diesel integrated microgrid in Aljouf region. IEEE Access 2020, 8, 57630–57645. [CrossRef]
- [13] Luo, Y.; Yang, D.; Yin, Z.; Zhou, B.; Sun, Q. Optimal configuration of hybrid-energy microgrid considering the correlation and randomness of the wind power and photovoltaic power. IET Renew. Power Gener. 2020, 14, 616–627. [CrossRef]
- [14] Yahaya, A.A.; Al-Muhaini, M.; Heydt, G.T. Optimal design of hybrid DG systems for microgrid reliability enhancement. IET Gener. Transm. Distrib. 2020, 14, 816–823. [CrossRef]
- [15] Samy, M.; Mosaad, M.I.; Barakat, S. Optimal economic study of hybrid PV-wind-fuel cell system integrated to unreliable electric utility using hybrid search optimization technique. Int. J. Hydrog. Energy 2021, 46, 11217–11231. [CrossRef]
- [16] Lamichhane, A.; Zhou, L.; Yao, G.; Luqman, M. LCL Filter based grid-connected photovoltaic system with battery energy storage. In Proceedings of the 2019 14th IEEE Conference on Industrial Electronics and Applications (ICIEA), Xi'an, China, 19–21 June 2019; Institute of Electrical and Electronics Engineers (IEEE): New York, NY, USA, 2019; pp. 1569–1574.
- [17] STH-215-P Solar Panel from 1Soltech Specifications. Available online: http://www.posharp.com/1sth-215-p-solar-panel-from 1soltech_p1621902445d.aspx (accessed on 25 July 2021).
- [18] Al-Mahmodi, M.; Al-Quraan, A. On-grid solar energy system—A study case in Irbid. In Proceedings of the 6th Global Conference on Renewable Energy and Energy Efficiency for Desert Regions (GCREEDER 2018), Amman, Jordan, 3–5 April 2018.
- [19] Rathore, A.; Patidar, N. Reliability assessment using probabilistic modelling of pumped storage hydro plant with PV-wind based standalone microgrid. Int. J. Electr. Power Energy Syst. 2019, 106, 17–32. [CrossRef]

- [20] Al-Quraan, A.; Stathopoulos, T.; Pillay, P. Comparison of wind tunnel and onsite measurements for urban wind energy estimation of potential yield. J. Wind. Eng. Ind. Aerodyn. 2016, 158, 1–10. [CrossRef].
- [21] Stathopoulos, T.; Alrawashdeh, H.; Al-Quraan, A.; Blocken, B.; Dilimulati, A.; Paraschivoiu, M.; Pilay, P. Urban wind energy: Some views on potential and challenges. J. Wind Eng. Ind. Aerodyn. 2018, 179, 146–157. [CrossRef]
- [22] 22. Yang, D.; Jiang, C.; Cai, G.; Huang, N. Optimal sizing of a wind/solar/battery/diesel hybrid microgrid based on typical scenarios considering meteorological variability. IET Renew. Power Gener. 2019, 13, 1446–1455. [CrossRef]